

Formation of Hydroxylamine (NH₂OH) in Electron-Irradiated Ammonia–Water Ices

Weijun Zheng^{†,‡,§} and Ralf I. Kaiser^{*,‡}

Institute for Astronomy and Department of Chemistry, University of Hawaii, Honolulu, Hawaii 96822, and State Key Laboratory of Molecular Reaction Dynamics, Institute of Chemistry, Chinese Academy of Sciences, Beijing 100190, P. R. China

Received: December 17, 2009; Revised Manuscript Received: February 10, 2010

We investigated chemical and physical processes in electron-irradiated ammonia–water ices at temperatures of 10 and 50 K. Chemically speaking, the formation of hydroxylamine (NH₂OH) was observed in electron-irradiated ammonia–water ices. The synthesis of molecular hydrogen (H₂), molecular nitrogen (N₂), molecular oxygen (O₂), hydrazine (N₂H₄), and hydrogen peroxide (H₂O₂), which was also monitored in previous irradiation of pure ammonia and water ices, was also evident. These newly formed species were trapped inside of the ices and were released into the gas phase during the warm-up phase of the sample after the irradiation. A quantitative analysis of the data showed that the production rates of the newly formed species at 10 K are higher compared to those at 50 K. Our studies also suggest that hydroxylamine is likely formed by the recombination of amino (NH₂) with hydroxyl (OH) radicals inside of the ices. Considering the physical effects on the ice sampled during the irradiation, the experiments provided compelling evidence that the crystalline ammonia–water ice samples can be partially converted to amorphous ices during the electron irradiation; similar to the chemical processes, the irradiation-induced amorphization of the ices is faster at 10 K than that at 50 K — a finding which is similar to electron-irradiated crystalline water ices under identical conditions. However, the amorphization of water in water–ammonia ices was found to be faster than that in pure water ices at identical temperatures.

1. Introduction

Ammonia has been reported to be present with an abundance of a few percent with respect to water on the surfaces of various icy bodies in the outer solar system, including Saturn's satellite Enceladus,^{1,2} Uranus's moon Miranda,³ Pluto's satellite Charon,^{4,5} and Kuiper Belt Object (50000) Quaoar.⁶ Ammonia might also exist on dust grains in cold molecular clouds with an abundance between 1 and 10% with respect to water.^{7–10} The ices in the cold molecular clouds and outer solar system are subjected to the irradiation by cosmic ray particles, ultraviolet (UV) photons, solar wind, and/or energetic particles trapped in planetary magnetospheres. It has been suggested that sputtering of ammonia might contribute to the abundance of molecular nitrogen (N₂) on Triton and Pluto;¹¹ also, the concentration of ammonia in the surface layers on the Saturnian satellites was proposed to be depleted by ion sputtering.^{12,13} Very recently, laboratory experiments implied that the nitrogen in Saturn's ring and the water vapor plume on Enceladus might result from the irradiation of an ammonia–water ice mixture on the surface of Enceladus.^{14,15} Irradiation exposures of ammonia–water ice have also been investigated with 0.8 MeV protons by Moore et al.¹⁶ at 10 and 80 K. However, chemically correct formation routes and the temperature-dependent yields of the detected molecules have remained highly speculative and elusive. These limited studies on the underlying chemistry of ammonia–water ices at different temperatures call for a systematic experimental study utilizing both infrared spectroscopy and mass spectrometry simultaneously to give detailed and complementary information

on the underlying chemical and physical processes during the irradiation of ammonia–water ices.

2. Experimental Section

The experiments were carried out in an ultrahigh vacuum chamber.¹⁷ A two-stage closed-cycle helium refrigerator coupled with a rotary platform is attached to the main chamber and holds a polished polycrystalline silver mirror serving as a substrate for the ice condensation. With the combination of the closed-cycle helium refrigerator and a programmable temperature controller, the temperature of the silver mirror can be regulated precisely to ± 0.3 K between 10 and 350 K. The ammonia–water ice mixtures were prepared by condensing anhydrous ammonia (99.99%, Matheson Gas Products, Inc.) and water vapor onto the silver mirror at 10 K as described in ref 18. Ammonia and water were introduced into the chamber simultaneously through two different capillaries (one for ammonia and the other for water). The angle between the capillaries was 55°, while the normal to the substrate bisected at that angle. The capillaries were located 4 cm away from the silver substrate. The background pressure in the main chamber was 7×10^{-11} Torr. Our ultrahigh vacuum conditions are crucial to eliminate any contamination effects which are observed when conducting irradiation experiments typically under high vacuum conditions of pressures higher than 10^{-8} Torr. During the condensation, the partial pressure of ammonia in the main chamber was maintained at 2.4×10^{-9} Torr, and that of water was at 2.0×10^{-8} Torr for about 20 min to prepare ammonia–water ices. We considered the nominal gas correction factors (H₂O: 1.12; NH₃: 1.23) when we determined the actual pressure based on the values shown by the ionization gauge since ionization gauges respond to water and ammonia differently. The total target thickness was determined to be 127 ± 15 nm, with an ammonia

* To whom correspondence should be addressed. E-mail: ralfk@hawaii.edu.

[†] Institute for Astronomy, University of Hawaii.

[‡] Department of Chemistry, University of Hawaii.

[§] Chinese Academy of Sciences.

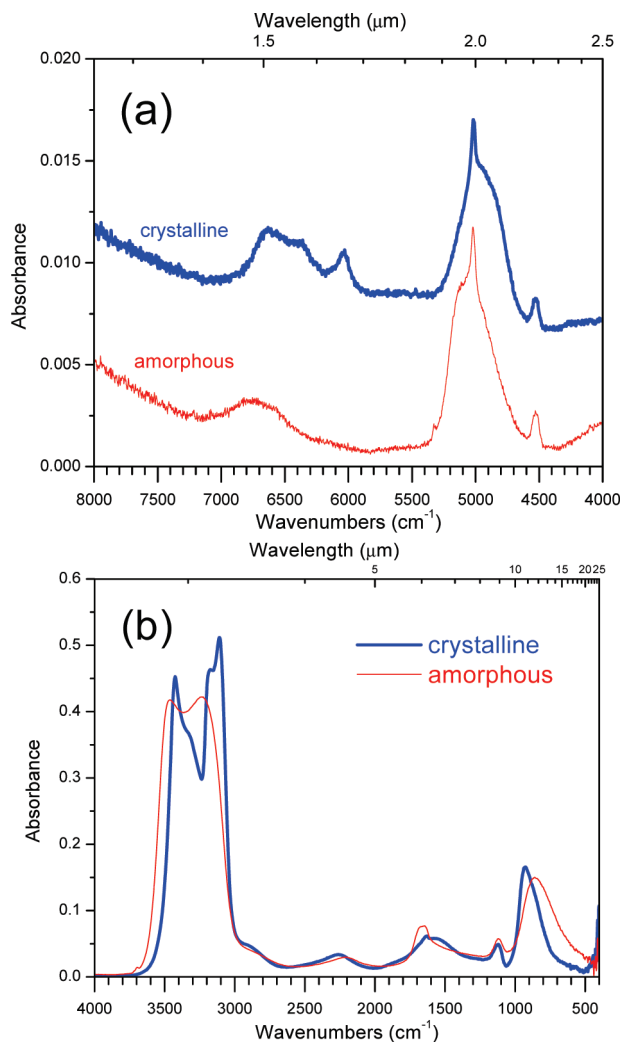


Figure 1. Infrared spectra of ammonia–water ice in the amorphous and crystalline phases (10 K).

fraction of $6.9 \pm 0.4\%$, as outlined previously.¹⁹ Considering the initial 10% ammonia–water gas mixture prepared for deposition, this indicates that in the deposited ices, the water molecule is enriched compared to the gas phase (fractionated condensation). The day-to-day reproducibility of the thicknesses has been determined to be 5%.

The ammonia–water ice mixtures condensed at 10 K were amorphous. They were heated to 130 K at 0.5 K min^{-1} for crystallization and then recooled to the desired temperatures (10 and 50 K). Figure 1 shows the infrared spectra of ammonia–water ice in the amorphous and crystalline phases. The crystalline samples were irradiated with 5 keV electrons for 180 min at electron currents of 0 (blank experiment) and 200 nA by scanning the electron beam over an area of $3.1 \pm 0.2 \text{ cm}^2$ utilizing a commercially available electron source (SPECS). It should be stressed that the electron current was monitored during the irradiation continuously; also, a feedback loop guaranteed that the electron current did not change during the irradiation. Utilizing the CASINO Code,²⁰ the penetration depth of 5 keV electrons in our ammonia–water ices was calculated to be $500 \pm 30 \text{ nm}$. Briefly, this computer program utilizes the kinetic energy, the target composition (chemical composition, density), and the target thickness as input parameters and calculates, for instance, the energy loss of the energetic electron while passing the solid-state target. Due to the water-rich matrix, it is not surprising that this penetration depth is similar to the penetration

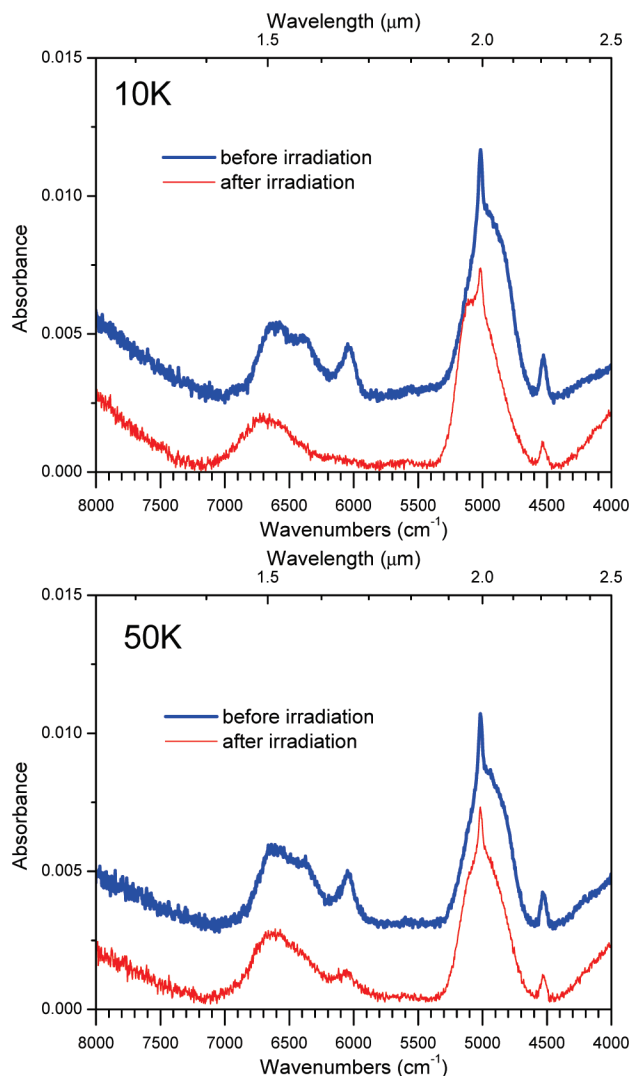


Figure 2. Near-IR spectra of ammonia–water ice before and after the irradiation.

of 5 keV electrons in pure water ices;¹⁷ it is important to stress that the penetration depth of the energetic electrons is much larger than the thickness of our samples; therefore, the electrons completely penetrate the water–ammonia ices. After the irradiation, the samples were kept at the same temperature for 60 min and were then warmed up at a speed of 0.5 K min^{-1} until all molecules sublimed from the ice into the gas phase. The infrared spectra of the samples were measured by a Fourier transform infrared spectrometer (Nicolet 6700 FTIR). A quadrupole mass spectrometer (Balzer QMG 420) monitored the species released into the gas phase (mass range: 1–200 amu).

3. Results

3.1. Infrared Spectra. Figures 2 and 3 show the near-IR and mid-IR spectra of the ammonia–water ices before and after the irradiation. At 10 K, the infrared spectra after the irradiation are similar to those of amorphous ice. The $1.65 \mu\text{m}$ (6060 cm^{-1}) band of crystalline ice decreased significantly after the irradiation. Also, the fine structure of the $3 \mu\text{m}$ (3300 cm^{-1}) band was destroyed by the irradiation. The changes in the 1.65 and $3 \mu\text{m}$ bands indicate that the crystalline ice was (partly) amorphized by the irradiation. At 50 K, some of the $1.65 \mu\text{m}$ band survived the irradiation. Further, the change in the $3 \mu\text{m}$ band is less pronounced compared to that at 10 K; this implies that the

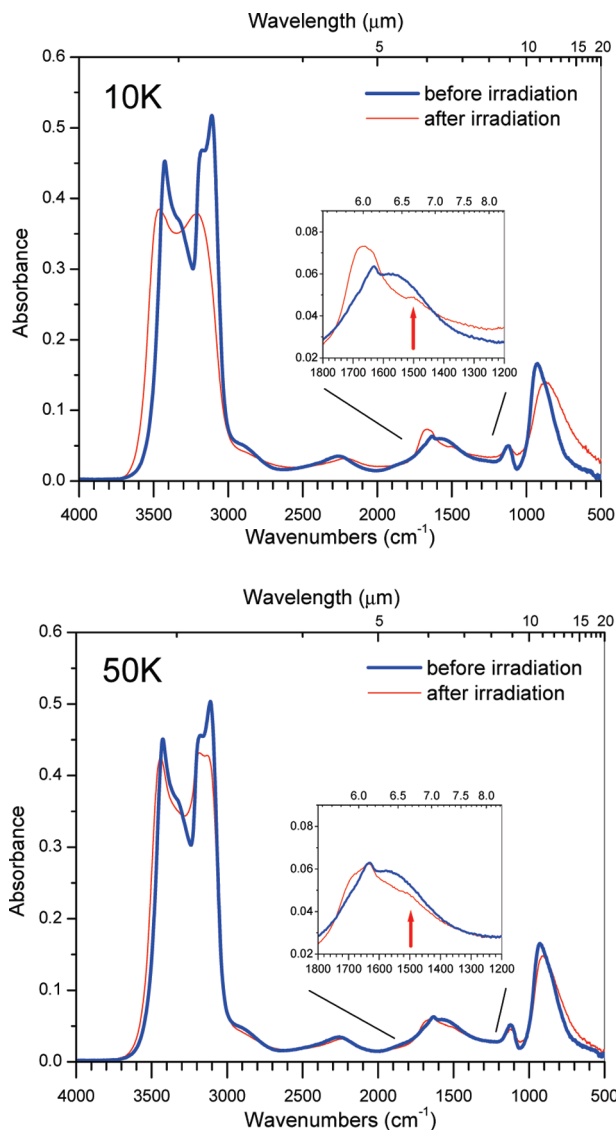


Figure 3. Mid-IR spectra of ammonia–water ice before and after the irradiation.

radiation-induced amorphization is incomplete at 50 K. This is consistent with the previous studies of pure water ice.^{19,21–24} Since the main topic of this paper is the radiation-induced chemistry in water–ammonia ices, we focus in the remaining section on the nature of the newly formed molecules (Figure 3). Here, we are able to identify a novel absorption peak at 1500 cm⁻¹ (6.67 μm), as pointed out by the arrow in Figure 3. Its intensity is weaker at 50 K compared to that at 10 K. A realistic assignment is due to the formation of [•]NH₂ radicals since the [•]NH₂ radical has an absorption peak at 1499 cm⁻¹ (6.67 μm).²⁵ This radical has also been observed in our laboratory in electron-irradiated pure ammonia ices.¹⁵ The absorption features of the newly formed hydroxylamine emerged only when the samples were warmed up to about 174 K, that is, at a temperature when most water and ammonia sublimed. Figure 4 shows the decay of these features during the warm-up of the postirradiation sample. The spectra in Figure 4 resulted from the irradiation at 10 K. The hydroxylamine features observed are summarized in Table 1. The same features were also monitored for the sample irradiated at 50 K, except they were much weaker, with an intensity of only 20% of that in the 10 K experiment.

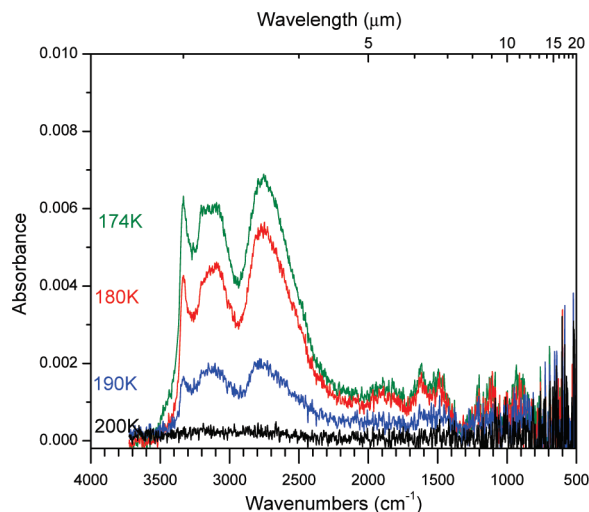


Figure 4. Absorption features of the products after ammonia and water sublimed.

TABLE 1: Infrared Absorption Features of the Newly Formed Hydroxylamine (NH₂OH) Observed in Figure 4

absorption, cm ⁻¹	literature value, cm ⁻¹		assignments
	gas ^a	solid ^b	
3332	3359	3302	NH ₂ OH ν ₇ (a'') antisym. N–H stretch
3209–3074	3294	3245	NH ₂ OH ν ₂ (a') sym. N–H stretch
2943–2507	2689	3173	ν ₃ + ν ₄
		2867	2ν ₄
		2787	ν ₃ + ν ₅
1886	1778	2675	ν ₄ + ν ₈
		1697	2ν ₆
		1675	
1616	1604	1564	NH ₂ OH ν ₃ (a') NH ₂ bend
1486	1353	1515	NH ₂ OH ν ₄ (a') NOH bend
1201	1294	1191	NH ₂ OH ν ₈ (a'') NH ₂ rock
1107	1115	950	NH ₂ OH ν ₅ (a') NH ₂ wag
921	895	912	NH ₂ OH ν ₆ (a') N–O stretch

^a References 29 and 30. ^b Reference 31.

Besides the chemical changes, we would also like to address briefly how the electron exposure affects the ices physically. At 10 K, the infrared spectra of the crystalline ice after the irradiation look similar to those of amorphous ice (Figure 2). The 1.65 μm (6060 cm⁻¹) band, which is characteristic of crystalline ice,¹⁹ decreased significantly after the irradiation. The changes in the 1.65 μm band indicate that the crystalline ice was (partly) amorphized during the irradiation. At 50 K, some of the 1.65 μm band survived the irradiation; this implies that the radiation-induced amorphization is incomplete at 50 K. This is consistent with the previous studies of pure water ice.¹⁹ Figure 5 plots the survival of the 1.65 μm band versus irradiation time at different temperatures. Here, α is the ratio between the surviving and original 1.65 μm band areas as defined in reference.¹⁹ Figure 5 indicates that the water ice in the ammonia–water mixture can be amorphized more efficiently than that in pure water ice at the same temperature. The amorphization of water in the ammonia–water ice reached equilibrium after about 30 min; in pure water ice, this process took about 3 h.¹⁹

3.2. Mass Spectra. We monitored the species released into the gas phase with a quadrupole mass spectrometer during and after the irradiation. The products released during the irradiation were below the detection limit of our system, that is, a partial pressure of 10⁻¹⁵ Torr. Here, we present the mass spectral results during warming of the ammonia–water ice. Figure 6a is from the blank experiment (no irradiation). Figure 6b resulted from the

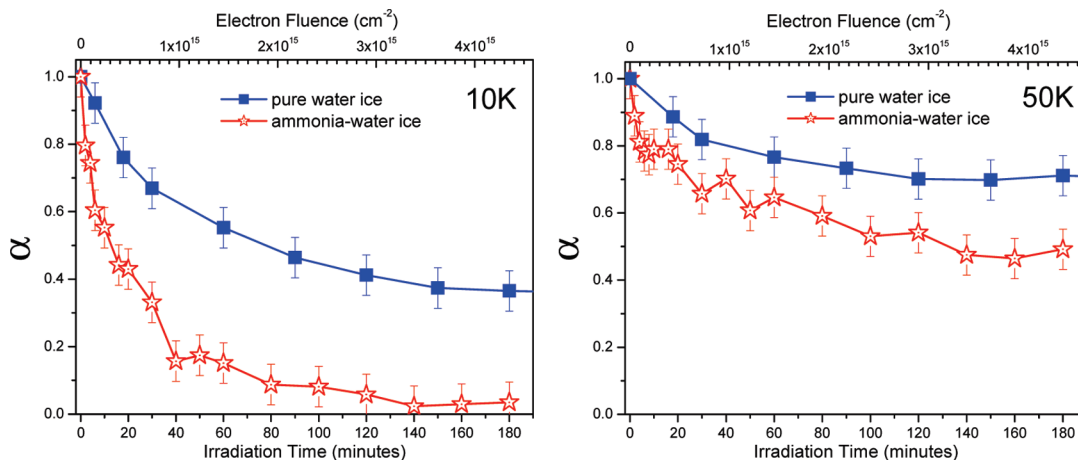


Figure 5. Survival of the $1.65 \mu\text{m}$ band versus the irradiation time at different temperatures. Here, α is the ratio between the surviving and original $1.65 \mu\text{m}$ band areas. The data of pure water ice are taken from ref 19.

sample irradiated with a 200 nA electron current at 10 K for 3 h. Comparison of Figure 6b to a shows that there is a new H_2 peak (monitored with $m/z = 2$) between 80 and 145 K; also, the intensity of N_2 ($m/z = 28$) between 130 and 172 K is higher than that in the blank experiment. This fact indicates that molecular hydrogen (H_2) and molecular nitrogen (N_2) have been generated by electron irradiation, trapped in the ice, and released to the gas phase upon warm-up. It might also be possible for some of the H_2 and N_2 to be formed during the warming-up process by combination of H and N atoms trapped in the ice. In addition to the formation of molecular hydrogen and molecular nitrogen, hydrogen peroxide (H_2O_2) and hydroxylamine (NH_2OH) were also detected (recall that hydroxylamine was also monitored via infrared spectroscopy). Hydrogen peroxide was released into the gas phase between 175 and 200 K. Hydroxylamine was detected between 160 and 200 K. The release of newly formed molecular oxygen (O_2) and hydrazine (N_2H_4) was monitored between 160 and 200 K. We could not separate O_2 and N_2H_4 since they have the same mass-to-charge ratio. In Figure 6c (irradiated at 50 K), molecular hydrogen, molecular nitrogen, and hydroxylamine were observed. The newly formed hydroxylamine (NH_2OH ; $m/z = 33$) was released into the gas phase between 160 and 180 K. Hydrogen peroxide was absent in the 50 K irradiation. In order to give an estimate of the product quantities, the ion currents of the newly formed molecules were integrated and, accounting for the pumping speed and molecular masses, converted to the number of molecules synthesized (N).¹⁷ The results are summarized in Table 2. The mass spectra show that the quantities of the new products are much lower in the 50 K experiment than those in the 10 K experiment, in agreement with the results from the infrared study. It is also consistent with our previous study of pure water ice.²⁶ Here, the formation of hydrogen peroxide (HOOH), molecular oxygen (O_2), and molecular hydrogen (H_2) dropped as the temperature increased.

4. Discussion and Conclusion

In the ammonia–water ice, an ammonia molecule can undergo unimolecular decomposition upon electron irradiation to form a hydrogen atom and an amino radical (reaction 1).¹⁵ Also, the unimolecular decomposition of a water (H_2O) was found to produce a hydroxyl (OH) plus a hydrogen atom (reaction 2).¹⁷ The hydrogen atoms can recombine to form molecular hydrogen via reaction 3.

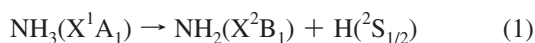
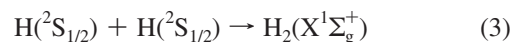
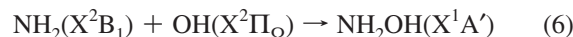
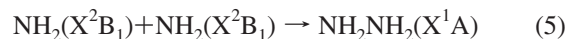


TABLE 2: Estimate of the Quantities of the New Species Produced in Ammonia–Water Ice by Electron Irradiation

	N , number of molecules	
	10 K	50 K
H_2	6.1×10^{16}	4.0×10^{16}
N_2	3.5×10^{15}	5.8×10^{14}
$\text{O}_2/\text{N}_2\text{H}_4$	$>4.2 \times 10^{14}$	$>2.4 \times 10^{14}$
NH_2OH	$>5.2 \times 10^{14}$	$>1.2 \times 10^{14}$
H_2O_2	$>2.3 \times 10^{14}$	>0



Hydrogen peroxide (H_2O_2) can be produced through the combination of two hydroxyl radicals (reaction 4), as also observed in irradiated pure water ices.¹⁷ Similarly, hydrazine (NH_2NH_2) can be formed via the combination of two NH_2 radicals (reaction 5); this process was also monitored in electron-irradiated neat ammonia samples at 10 K.¹⁵ Hydroxylamine (NH_2OH) is likely synthesized through the reaction between an amino radical and a hydroxyl radical in an exothermic reaction (reaction 6, $\Delta H_{r,298}^0 = -278 \text{ kJ mol}^{-1}$).²⁷



Our experiments support the previous work that ammonia in the surface of the Saturnian satellites can be partially converted to hydroxylamine by irradiation.^{12,13} Loeffler et al.¹⁴ proposed that an irradiation of the ammonia–water ice on Enceladus might be responsible for a larger concentration of N^+ and N_2 in the Saturn's E-ring, and the plume of gas and particles from the South Polar region of Enceladus might be due to the irradiation generation of hydrogen and nitrogen. Since molecular hydrogen is a major product generated by irradiation in ammonia–water ice, a larger concentration of hydrogen should also be detected if the nitrogen in the inner magnetosphere of Saturn originated from the ammonia–water ice on Enceladus. In addition, our

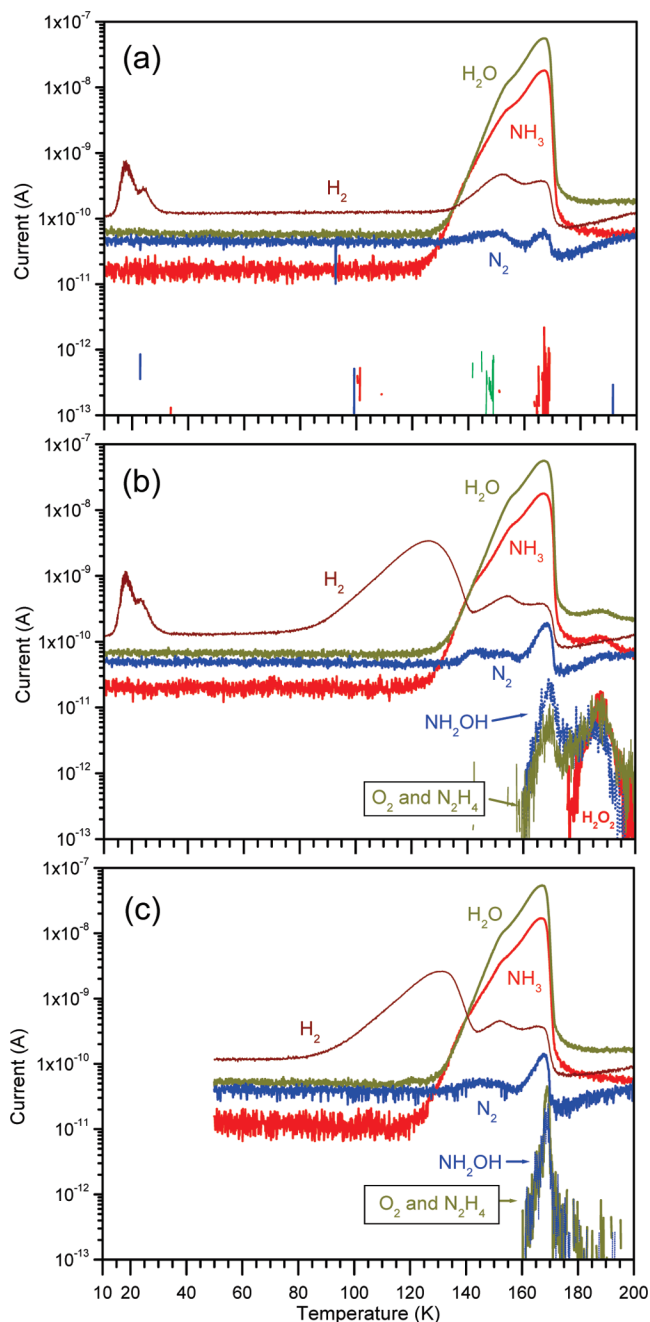


Figure 6. The temporal evolution of the ion currents during the warm-up of the samples; (a) no irradiation, (b) irradiated at 10 K, (c) irradiated at 50 K.

experiments suggest that hydroxylamine (NH₂OH) exists in the surface of those objects where ammonia has been found. However, hydroxylamine in water-rich ices might be undetectable via the infrared method because its absorption features are hidden in the strong bands of water ice. According to our knowledge, there is no report of hydroxylamine in molecular clouds or in the outer solar system — neither in the solid state nor in the gas phase. It might be detectable with microwave spectroscopy in the gas phase, where the temperature is higher than 160 K and all of the hydroxylamine has sublimed into the gas phase. Our experiments also showed that the concentration of newly formed hydrogen peroxide in irradiated water ice can

be reduced due to the existence of ammonia. If a high concentration of hydrogen peroxide can be detected on an object, the concentration of ammonia on that object probably is very low. Note that the LETs (linear energy transfer) of a 5 keV electron in 127 ± 15 nm thick ammonia–water ice (0.9 g cm^{-3}) simulated with CASINO²⁰ are $6.5 \pm 1.5 \text{ keV } \mu\text{m}^{-1}$; we estimated that the actual dose in our experiment in 3 h is between $10 \pm 2 \text{ eV}$ per molecule. This dose is similar to the dose on the surface of a Kuiper belt object in 10^8 years ($\sim 10 \text{ eV}$ per molecule).²⁸ Therefore, our experiments provide crucial guidance to the absolute formation rates of hydroxylamine in the surfaces of KBOs.

Acknowledgment. This work was financed by the U.S. National Science Foundation (NSF; AST-0507763; R.I.K.) and by the NASA Astrobiology Institute under Cooperative Agreement NNA04CC08A at the University of Hawaii–Manoa (W.Z.). We are grateful to Ed Kawamura (University of Hawaii at Manoa, Department of Chemistry) for his electrical work.

References and Notes

- (1) Verbiscer, A. J.; Peterson, D. E.; Skrutskie, M. F.; Cushing, M.; Helfenstein, P.; Nelson, M. J.; Smith, J. D.; Wilson, J. C. *Icarus* **2006**, *182*, 211.
- (2) Emery, J. P.; Burr, D. M.; Cruikshank, D. P.; Brown, R. H.; Dalton, J. B. *Astron. Astrophys.* **2005**, *435*, 353.
- (3) Bauer, J. M.; Roush, T. L.; Geballe, T. R.; Meech, K. J.; Owen, T. C.; Vacca, W. D.; Rayner, J. T.; Jim, K. T. C. *Icarus* **2002**, *158*, 178.
- (4) Brown, M. E.; Calvin, W. M. *Science* **2000**, *287*, 107.
- (5) Dumas, C.; Terrile, R. J.; Brown, R. H.; Schneider, G.; Smith, B. A. *Astron. J.* **2001**, *121*, 1163.
- (6) Jewitt, D. C.; Luu, J. *Nature* **2004**, *432*, 731.
- (7) Maret, S.; Bergin, E. A.; Lada, C. J. *Nature* **2006**, *442*, 425.
- (8) Greenberg, J. M.; van de Bult, C. E. P. M.; Allamandola, L. J. *J. Phys. Chem.* **1983**, *87*, 4243.
- (9) Dartois, E.; d'Hendecourt, L. *Astron. Astrophys.* **2001**, *365*, 144.
- (10) Gibb, E. L.; Whittet, D. C. B.; Chiar, J. E. *Astrophys. J.* **2001**, *558*, 702.
- (11) Johnson, R. E. *Sputtering and Desorption from Icy Surfaces. In Solar System Ices*; ASSL Series; Kluwer Academic Publishers: Dordrecht, The Netherlands, 1998; Vol. 227, p 303.
- (12) Lanzerotti, L. J.; Brown, W. L.; Marcantonio, K. J.; Johnson, R. E. *Nature* **1984**, *312*, 139.
- (13) Strazzulla, G.; Palumbo, M. E. *Planet. Space Sci.* **1998**, *46*, 1339.
- (14) Loeffler, M. J.; Raut, U.; Baragiola, R. A. *Astrophys. J.* **2006**, *649*, L133.
- (15) Zheng, W.; Jewitt, D.; Osamura, Y.; Kaiser, R. I. *Astrophys. J.* **2008**, *674*, 1242.
- (16) Moore, M. H.; Ferrante, R. F.; Hudson, R. L.; Stone, J. N. *Icarus* **2007**, *190*, 260.
- (17) Zheng, W.; Jewitt, D.; Kaiser, R. I. *Astrophys. J.* **2006**, *639*, 534.
- (18) Zheng, W.; Jewitt, D.; Kaiser, R. I. *Astrophys. J. Suppl. Ser.* **2009**, *181*, 53.
- (19) Zheng, W. J.; Jewitt, D.; Kaiser, R. I. *J. Phys. Chem. A* **2009**, *113*, 11174.
- (20) Hovington, P.; Drouin, D.; Gauvin, R. *Scanning* **1997**, *19*, 1.
- (21) Mastrapa, R. M. E.; Brown, R. H. *Icarus* **2006**, *183*, 207.
- (22) Baratta, G. A.; Spinella, F.; Leto, G.; Strazzulla, G.; Foti, G. *Astron. Astrophys.* **1991**, *252*, 421.
- (23) Strazzulla, G.; Baratta, G. A.; Leto, G.; Foti, G. *Europhys. Lett.* **1992**, *18*, 517.
- (24) Leto, G.; Baratta, G. A. *Astron. Astrophys.* **2003**, *397*, 7.
- (25) Milligan, D. E.; Jacox, M. E. *J. Chem. Phys.* **1965**, *43*, 4487.
- (26) Zheng, W.; Jewitt, D.; Kaiser, R. I. *Astrophys. J.* **2006**, *648*, 753.
- (27) Fagerstrom, K.; Jodkowski, J. T.; Lund, A.; Ratajczak, E. *Chem. Phys. Lett.* **1995**, *236*, 103.
- (28) Cooper, J. F.; Christian, E. R.; Richardson, J. D.; Wang, C. *Earth, Moon, Planets* **2003**, *92*, 261.
- (29) Luckhaus, D. *J. Chem. Phys.* **1997**, *106*, 8409.
- (30) Kowal, A. T. *Spectrochim. Acta, Part A* **2002**, *58*, 1055.
- (31) Nightingale, R. E.; Wagner, E. L. *J. Chem. Phys.* **1954**, *22*, 203.